E2-2001-207

G.N.Afanasiev*, V.G.Kartavenko, V.P.Zrelov

PECULIARITIES OF CHERENKOV-LIKE RADIATION FROM THE DECELERATED ELECTRON ARIZING FROM THE β-DECAY IN WATER

Submitted to «Nuclear Instruments and Methods A»

[1]E-mail: afanasev@thsun1.jinr.ru

1 Introduction

Theoretically, when considering the Cherenkov radiation, one treats either the unbounded charge motion with a constant velocity (this corresponds to the so-called Tamm-Frank problem [1]) or the charge motion on a finite interval with an instantaneous acceleration and deceleration of a charge at the beginning and termination of its motion. This corresponds to the so-called Tamm problem [2]. The physical justification for the Tamm problem is as follows. A uniformly moving charge moves initially in vacuum (where it does not radiate), then penetrates into a transparent dielectric slab (where it radiates if the condition $\cos\theta_{Ch} = 1/\beta n$ for the Cherenkov angle is satisfied) and, finally, after leaving the dielectric slab, moves again in vacuum without radiating (we disregard the transition radiation at the boundaries of a dielectric slab). Since Tamm's problem is more physical than the Tamm-Frank one, it is frequently used for the analysis of experimental data (see e.g., [3-6]). However, the following complication arises. The superposition of electromagnetic fielda (EMFs) arising from the instantaneous acceleration and deceleration at the beginning and termination of a charge motion strongly resembles the Cherenkov radiation spectrum. This fact was first noted by S. Vavilov ([7]) (who was a Cherenkov teacher). We quote him (our translation from Russian):

> "We think that the most probable reason for the γ- luminiscence is the radiation arising from the deceleration of Compton electrons. The hardness and intensity of γ rays in the experiments of P.A. Cherenkov were very large. Therefore, the number of Compton scattering events and the number of scattered electrons should be very considerable in fluids. The free electrons in a dense fluid should be decelerated at negligible distances. This should be followed by the radiation of the continuous spectrum. Thus, a weak visible radiation may arise, although the boundary of bremsstrahlung and its maximum should be located somewhere in the Roentgen region. It follows from this that the energy distribution in the visible region should rise towards the violet part of the spectrum, and the blue-violet part of the spectrum should be especially intensive".

This Vavilov explanation of the Cherenkov effect has given rise to a number of attempts [8,9] in which the observed radiation originating from a charge passage through the dielectric slab was attributed to the interference of bremsstrahlung (BS) shock waves. On the other hand, the exact solution of the Tamm problem in a nondispersive medium was found and analyzed in [10]. It was shown there that the Cherenkov shock wave exists side by side with BS shock waves and not in any case can be reduced to them. Then, how this fact can be reconciled with the results of [8, 9] which describe experimental data quite satisfactorily? A possible reason is that the exact solution obtained in [10] was written in the space-time representation, while the authors of [8,9] operated with the Tamm formula related to the frequency representation. It might happen that the main contribution to the exact solution

of [10] describing the Cherenkov wave is due to the integration over the frequency region lying outside the visible part of the intensity spectrum. Then, the radiation in the visible part of spectrum could be described by the Tamm formula.

The aim of this consideration is to consider the electromagnetic radiation arising from an instant acceleration of a charge followed by its smooth deceleration. The charge motion begins with some velocity v and lasts up to its complete stopping. Formerly, the decelerated charge motion with a rather small change of velocity was studied analytically and numerically in Refs. [11, 12]. In the present consideration, the change of velocity is so large that analytical formulae used in [11, 12] do not work. Numerically, the charge motion with small and arbitrary changes of velocity was studied in [13] and [14], resp. However, the consideration of [14] was mainly of methodological nature, without taking account of realistic conditions.
To clarify the peculiarities of the Cherenkov-like radiation from the β-decayed electron, we take into account only its deceleration and deliberately exclude such effects as multiple scattering. These effects, albeit being quantitatively important, obscure the influence of deceleration on the direction of radiation given by the Tamm-Frank formula $\cos\theta = 1/\beta n$. We assume the medium to be continuous and postulate that the whole energy loss takes place on a path defined by Tables available in physical literature.

The plan of our exposition is as follows. The formulation of the treated problem is given in section 2. The main mathematical formulae needed for subsequent calculations are presented in section 3. Numerical results are collected in section 4. A brief discussion of the results obtained is given in section 5.

2 Statement of the problem

We consider the following problem. A point charge is at rest in a medium at the origin up to a moment $t = 0$. At this moment, the charge exhibits the instant acceleration, acquiring the velocity v_0. Then, the charge moves with a constant deceleration along the z axis, After the moment $t = t_f$, the velocity of the charge is zero, i.e., it is again at rest at the point $z = z_f$ of the z axis.
We choose the motion law in the form

$$z(t) = v_0 t - \frac{1}{2} a t^2. \tag{2.1}$$

The charge velocity is

$$v(t) = \frac{dz}{dt} = v_0 - at. \tag{2.2}$$

The charge velocity vanishes at the moment of time $t_f = v_0/a$. At this moment the charge position is $z_f = v_0^2/2a$. It is convenient to operate not with acceleration a, but with the distance z_f passed by the charge up to its complete stopping (it can be found from the Tables [15]). Then, a can be expressed through z_f and v_0:

$$a = v_0^2/2z_f. \tag{2.3}$$

From (2.1) we express the current time through the charge position at this moment

$$t = \frac{2z_f}{v_0}(1 - \sqrt{1 - z/z_f}). \tag{2.4}$$

Substituting (2.4) into (2.2), we find the charge velocity as a function of its velocity:

$$v = v_0\sqrt{1 - z/z_f}. \tag{2.5}$$

The dependence $v(z)$ given by (2.5) is not very realistic. The realistic dependence should be exctracted from the relation (see, e.g., [16])

$$\frac{d\mathcal{E}}{dz} = -\frac{C}{v^2},$$

where C is a function weakly dependent of the current charge velocity v, $\mathcal{E}$ is the relativistic cinetic energy ($\mathcal{E} = m_0c^2(\gamma - 1)$, $\gamma = (1-\beta^2)^{-1/2}$, $\beta = v/c$). However, our main task is to clarify how the charge acceleration affects the angular-frequency distribution of the radiated energy. For this purpose, the simplified version of the velocity loss (2.5) is quite enough.

3 Main mathematical formulae

We intend here to find the electromagnetic field and the energy flux arising from the motion law (2.1). The current density corresponding to (2.1) equals

$$j_z = e(v_0 - at)\delta(x)\delta(y)\delta(z - v_0t + at^2/2) \tag{3.1}$$

in the time interval $0 < t_< t_f$ and is zero outside it. The Fourier component of this current density is given by

$$j_\omega = \frac{1}{2\pi}\int_0^{t_f} \exp(-i\omega t)j_z(t)dt = \frac{e}{2\pi}\delta(x)\delta(y)\exp[-\frac{i\omega v_0}{a}(1 - \sqrt{1 - z/z_f})] \tag{3.2}$$

for $0 < z < z_f$ and $j_\omega = 0$ outside this interval.

The Fourier component of the vector potential is

$$A_z(\omega) = \frac{e\mu}{2\pi c}\int \frac{dz'}{R}\exp(-i\psi), \tag{3.3}$$

where

$$\psi = \frac{\omega v_0}{a}(1 - \sqrt{1 - z'/z_f}) + k_nR, \quad k_n = n\omega/c, \quad R = [r^2 + z'^2 - 2rz'\cos\theta]^{1/2}, \tag{3.4}$$

ϵ and μ are electric and magnetic permittivities of the medium, $n = \sqrt{\epsilon\mu}$ is its refractive index, r is the distance from the origin to the observation point, θ is its

polar angle. For simplicity, we limit ourselves to the nonmagnetic medium ($\mu = 1$). The sole non-vanishing component of magnetic field is H_ϕ:

$$H_\omega = \frac{iek_n r}{2\pi c} \sin\theta \int \frac{dz'}{R^2} \exp(-i\psi). \tag{3.5}$$

The electric field strength is obtained from the Maxwell equation

$$curl\vec{H} = \frac{\epsilon}{c}\frac{\partial \vec{E}}{\partial t}$$

valid outside the motion interval. In the Fourier representation, this equation looks as

$$curl\vec{H} = \frac{i\omega\epsilon}{c}\vec{E}.$$

Due to the axial symmetry of the problem, only the θ component of $\vec{E}$ differs from zero

$$E_\omega = \frac{ic}{\omega\epsilon r}\frac{\partial}{\partial r}(rH_\omega) = \frac{iekr\sin\theta}{2\pi c}\int \frac{r - z'\cos\theta}{R^3}\exp(-i\psi)dz'. \tag{3.6}$$

When obtaining (3.5) and (3.6), the terms of the order $1/k_n R$ were dropped outside sine and cosine functions. Usually, they are of the order 10^{-7}.

The radial energy flux through the unit solid angle of the sphere with the radius r for the whole time of charge motion is given by

$$S_r(\theta) = \frac{cr^2}{4\pi}\int_{-\infty}^{\infty} E_\theta(t)H_\phi(t)dt.$$

Inserting here

$$E_\theta(t) = \int \exp(i\omega t)E_\omega d\omega \quad \text{and} \quad H_\phi(t) = \int \exp(i\omega t)H_\omega d\omega,$$

one gets

$$S_r(\theta) = \int_0^\infty S_r(\theta,\omega)d\omega,$$

where

$$S_r(\theta,\omega) = cr^2[E_r(\omega)H_r(\omega) + E_i(\omega)H_i(\omega)]. \tag{3.7}$$

Subscripts of E and H mean real and imaginary parts of E_ω and H_ω. The latter are given by

$$H_r = \frac{ek_n r\sin\theta}{2\pi c}\int \frac{\sin\psi}{R^2}dz', \quad H_i = \frac{ek_n r\sin\theta}{2\pi c}\int \frac{\cos\psi}{R^2}dz',$$

$$E_r = \frac{ekr\sin\theta}{2\pi c}\int \frac{r - z'\cos\theta}{R^3}\sin\psi dz', \quad E_i = \frac{ekr\sin\theta}{2\pi c}\int \frac{r - z'\cos\theta}{R^3}\cos\psi dz'. \tag{3.8}$$

Here the z' integration is performed over the interval $(0, z_f)$. From (3.7) and (3.8) one gets

$$S_r(\theta,\omega) = \frac{d^2\mathcal{E}}{d\omega d\Omega} = \frac{e^2k^2nr^4\sin^2\theta}{4\pi^2c}\times$$
$$\times[\int \frac{\sin\psi}{R^2}dz' \cdot \int \frac{r - z'\cos\theta}{R^3}\sin\psi dz' + \int \frac{\cos\psi}{R^2}dz' \cdot \int \frac{r - z'\cos\theta}{R^3}\cos\psi dz')]. \tag{3.9}$$

It is convenient to pass to the dimensionless variable $z' \to z'/z_f$. Then,

$$S_r(\theta,\omega) = \frac{e^2k^2nz_f^2\sin^2\theta}{4\pi^2c}S, \tag{3.10}$$

where

$$S = \int \frac{\sin\psi}{R^2}dz' \cdot \int \frac{1 - \epsilon_f z'\cos\theta}{R^3}\sin\psi dz' + \int \frac{\cos\psi}{R^2}dz' \cdot \int \frac{1 - \epsilon_f z'\cos\theta}{R^3}\cos\psi dz'. \tag{3.11}$$

Here the z' integration is performed over the interval $(0, 1)$. Further,

$$\epsilon_f = z_f/r, \quad R = (1 + \epsilon_f^2 z'^2 - 2\epsilon_f z'\cos\theta)^{1/2}, \quad \psi = \frac{\omega v_0}{a}(1 - \sqrt{1 - z'}) + k_n r R.$$

Equation (3.11) is not very convenient, since for large frequencies, $\sin\psi$ and $\cos\psi$ are fast oscillating functions. For example, for the middle of optical diapason ($\lambda = 2\pi c/\omega \approx 6 \cdot 10^{-5} cm$) and the observation distance $r \approx 1m$, the value of $k_n r$ is of the order 10^7. To avoid this difficulty, we present ψ in the form

$$\psi = \psi_1 + k_n r, \quad \text{where} \quad \psi_1 = \omega\tau(z') + k_n r(R-1), \quad \tau(z') = \frac{2z_f}{v_0}(1 - \sqrt{1 - z'}). \tag{3.12}$$

Then, S in (3.10) can be written as

$$S_1 = \int \frac{\sin\psi_1}{R^2}dz' \cdot \int \frac{1 - \epsilon_f z'\cos\theta}{R^3}\sin\psi_1 dz' + \int \frac{\cos\psi_1}{R^2}dz' \cdot \int \frac{1 - \epsilon_f z'\cos\theta}{R^3}\cos\psi_1 dz'. \tag{3.13}$$

Finally, the radial intensity is

$$S_r(\theta,\omega) = \frac{e^2k^2nz_f^2\sin^2\theta}{4\pi^2c}S_1, \tag{3.14}$$

where S_1 is given by (3.13).

Equation (3.14) is more convenient for high frequencies than (3.10), since ψ_1 is of the order $k_n z_f$ when the motion interval is much smaller than the observation distance ($z_f << r$).

Let the observation sphere radius r be so large, that one can change R by r outside the ψ_1 function and retain in the development of R (inside the ψ_1 function) only the terms of the first order in z'. Then,

$$\psi_1 = \tau(z') - knz' \cos\theta. \tag{3.15}$$

In this case, the radiation intensity can be obtained in analytic form. But at first, consider more general problem which describes a charge moving on the interval z_1, z_2 according to the law

$$z = z_1 + v_1(t - t_1) + \frac{1}{2}a(t - t_1)^2. \tag{3.16}$$

The motion begins at the moment t_1 and terminates at the moment t_2. The charge velocity varies linearly with time from the value $v = v_1$ at $t = t_1$ up to value $v = v_2$ at $t = t_2$: $v = v_1 + a(t - t_1)$. Again, we express the acceleration a and the motion interval through z_1, z_2, v_1, v_2:

$$a = \frac{v_1^2 - v_2^2}{2(z_1 - z_2)}, \quad t_2 - t_1 = \frac{2(z_2 - z_1)}{v_2 + v_1}.$$

In this case, the function $\tau(z)$ entering into (3.16) is given by

$$\tau(z) = t_1 - 2v_1 \frac{z_2 - z_1}{v_2^2 - v_1^2}[1 - (1 + \frac{z - z_1}{z_2 - z_1}\frac{v_2^2 - v_1^2}{v_1^2})^{1/2}]. \tag{3.17}$$

The radial component of the radiation intensity is equal to

$$S_r(\theta, \omega) = \frac{e^2 k^2 n \sin^2\theta}{4\pi^2 c}[(\int_{z_1}^{z_2} dz' \cos\psi_1)^2 + (\int_{z_1}^{z_2} dz' \sin\psi_1)^2] =$$

$$= \frac{e^2 \sin^2\theta}{2\pi^2 cn \cos^2\theta}\{1 - \cos(u_2^2 - u_1^2) + \pi\alpha^2[(C_2 - C_1)^2 + (S_2 - S_1)^2] -$$

$$-\sqrt{2\pi}\alpha[(C_2 - C_1)(\sin u_2^2 - \sin u_1^2) - (S_2 - S_1)(\cos u_2^2 - \cos u_1^2)]\}, \tag{3.18}$$

where we put

$$C_1 = C(u_1), \quad C_2 = C(u_2), \quad S_1 = S(u_1), \quad S_2 = S(u_2),$$

$$\alpha = [\frac{k(z_2 - z_1)}{n|\cos\theta(\beta_2^2 - \beta_1^2|}]^{1/2}, \quad u_1 = \alpha(1 - \beta_1 n \cos\theta), \quad u_2 = \alpha(1 - \beta_2 n \cos\theta),$$

C and S are the Fresnel integrals defined as

$$S(x) = \sqrt{\frac{2}{\pi}}\int_0^x dt \sin t^2 \quad \text{and} \quad C(x) = \sqrt{\frac{2}{\pi}}\int_0^x dt \cos t^2.$$

When $v_2 \to v_1 = v$, the intensity (3.17) goes into the Tamm formula:

$$\sigma_T(\theta) = \frac{e^2}{\pi^2 cn}[\sin\theta \frac{\sin\omega t_0(1-\beta_n\cos\theta)}{\cos\theta - 1/\beta_n}]^2, \quad t_0 = \frac{z_2 - z_1}{v} \quad \beta_n = \frac{v}{c_n}. \tag{3.19}$$

Turning to the treated case with the final velocity equal to zero, we put $v_1 = v_0$, $v_2 = 0$, $t_1 = 0$, $t_2 = t_f$, $z_1 = 0$ and $z_2 = z_f$. Then, the same expression (3.18) for the radiation intensity holds in which one should put

$$u_1 = \alpha(1 - \beta_0 n\cos\theta), \quad u_2 = \alpha, \quad \alpha = \frac{1}{\beta_0}\sqrt{\frac{kz_f}{n|\cos\theta|}}, \quad \beta_0 = v_0/c.$$

4 Numerical calculations

Since Eq.(3.14) has a rather complicated analytic structure, we performed numerical calculations for the radiation generated by decelerated electrons with the maximal energy 10 MeV and for the radiation produced by decelerated electrons which arise from the β-decay of ^{40}K. The radius of the observation sphere was chosen to be $r = 100cm$. In realistic cases, we cannot expand $R - 1$ up to the terms of the first order in z':

$$R - 1 \sim -\epsilon_f z' \cos\theta,$$

which is the usual procedure when treating the Tamm model. In fact, the next-order terms in the expansion of $R - 1$ are of the order $\epsilon_f^2 z'^2$. According to (3.12), their contribution to the phase ψ_1 is of the order $2\pi z_f^2/4\lambda r$. For $\lambda = 4 \cdot 10^{-5}cm$, $z_f = 0.5cm$ and $r = 100cm$, this quantity is about 100. On the other hand, the contribution of these terms to ψ_1 can be disregarded if they are much smaller than unity (since ψ_1 is a phase). Therefore, second-order terms in the development of $R - 1$ are essential. For smaller distances their role increases. These questions were considered in greater detail in [12].

We consider the decelerated motion of electrons in water. For a given initial velocity v_0 of an electron, the ranges of electrons were taken from Tables [15]. In Table 1, we collected the electron ranges for those kinetic energies, for which calculations were made. For a given wavelength λ, the refractive index n was approximated by the formula

$$n(\lambda)|_{T=20^0C} = 1.32533 + \frac{2.5814 \cdot 10^{-11}}{\lambda^2} + \frac{4.588 \cdot 10^{-21}}{\lambda^4},$$

where λ is in cm. This approximation is in good agreement with the data given in [17]. In Table 2, we give the wavelengths λ, for which calculations were made together with their refractive indices $n(\lambda)$ and the threshold velocities $\beta_c = 1/n(\lambda)$. For the wavelength $\lambda = 5.893 \cdot 10^{-4}cm$ and $n = 1.333$, the angular distributions for various initial velocities are presented in the left column of Fig.1. Side by side with

deceleration motion curves, there are shown Tamm angular intensities

$$S_T = \frac{d^2\mathcal{E}}{d\Omega d\omega} = \frac{e^2}{\pi^2 cn}\{\sin\theta \frac{\sin[\omega L(1-\beta n\cos\theta)/2v]}{cos\theta - 1/\beta n}\}^2, \tag{4.1}$$

where for L and v we take the total path z_f and the initial velocity v_0. To make possible their comparison with angular intensities corresponding to the decelerated motion, we averaged Tamm intensities over 5 neighbouring points. Non-averaged Tamm intensities are presented in the right part of Fig. 1.

For the sufficiently large velocity $\beta = 0.959$ (this corresponds to $\beta n \approx 1.278$), the maximum of the angular distribution (3.14) is approximately at $\theta_m = 38.2^0$ (top of the left column of Fig. 1), while the usual formula for the Cherenkov angle $\theta_{Ch} = \arccos(1/\beta n)$ gives $\theta_{Ch} = 38.56^0$ which is by 0.3^0 smaller than θ_m. However, for β close to the threshold ($\beta = 1/n$), the shift of maxima is $\approx 3^0$ (middle of the left column of Fig. 1). It follows from Table 3 that the dependence $\theta_m(\beta)$ differs from that given by $\theta_{Ch} = \arccos(1/\beta n)$.

The third curve in Fig.1 (bottom of the left column) corresponds to the initial velocity $\beta_0 = 0.6593$ ($\beta_0 n = 0.927$) smaller than the light velocity in medium.

It should be kept in mind that the Tamm formula (4.1) is not applicable for the treated deceleration. In fact, Tamm [2] gives the following condition for the validity of (4.1):

$$\frac{t_0^2}{2}\frac{dv}{dt} << \lambda, \quad t_0 = \frac{L}{2v_0}. \tag{4.2}$$

In the present case,

$$\frac{dv}{dt} = a = v_0^2/2z_f, \quad t_0 = t_f/2 = z_f/v_0.$$

Therefore, (4.2) reduces to

$$z_f << \lambda.$$

If for λ we choose the middle of the optical diapason ($\lambda = 6\cdot 10^{-5} cm$) and for z_f we take the typical value $10^{-2} cm$, then (4.2) reduces to

$$10^{-2} << 6\cdot 10^{-5}.$$

Therefore, (4.2) is strogly violated and the Tamm formula should not work. Formerly, this was admitted in [13].

Deceleration motion intensities (left column) and the Tamm ones are shown in Fig.2 for the wavelength $\lambda = 5.893\cdot 10^{-5} cm$ in a smaller angular interval (in the neighborhood of the Cherenkov peak).

To see how the angular distributions change when the initial velocity v_0 changes from $v_0 > c/n$ to a value smaller than c/n, we present, in Fig.3, the radiation intensities for intermediate values of initial velocities. It is seen that the transition through the Cherenkov threshold is sufficiently smooth.

In Fig. 4 (a, b, c), we present angular distributions for three different initial velocities ($\beta_0 = 0.9594$, $\beta_0 = 0.7765$ and $\beta_0 = 0.6953$). For each of these velocities there are shown intensities for the wavelengths $\lambda = 2.144 \cdot 10^{-5} cm$ (solid curve), $\lambda = 3.034 \cdot 10^{-5} cm$ (broken curve) and $\lambda = 6.780 \cdot 10^{-5} cm$ (dotted curve). It is seen that the radiation intensity grows with diminishing the wavelength. The location of maxima of intensity angular distributions corresponding to the treated decelerated motion is close to that given by the Tamm formula (4.1) (see Table 3), although their forms differ appreciably.

The number of photons integrated over the solid angle is given by

$$\frac{dN}{d\lambda} = \frac{2\pi n \alpha z_f^2}{\lambda^3} \int_0^\pi S_1 \sin^3\theta d\theta, \tag{4.3}$$

where S_1 is given by (3.13) and $\alpha = e^2/\hbar c = 1/137$ is a fine structure constant.

The distribution $dN/d\lambda$ as a function of the observed wavelength λ, is shown in Fig. 5 (solid lines) for various initial charge velocities. In the same figure, there are presented Tamm's photon numbers (dotted lines) given by

$$\frac{dN_T}{d\lambda} = \frac{2\pi\alpha z_f}{\lambda^2}(1 - \frac{1}{\beta^n n^2}) + \frac{4\alpha}{\pi\lambda n}(\frac{1}{2\beta n} \ln \frac{1+\beta n}{\beta n - 1} - 1)$$

for $\beta n > 1$ and

$$\frac{dN_T}{d\lambda} = \frac{4\alpha}{\pi\lambda n}(\frac{1}{2\beta n} \ln \frac{1+\beta n}{1-\beta n} - 1) \tag{4.4}$$

for $\beta n < 1$. In all cases, Tamm intensities for $v > c/n$ are much larger than those corresponding to the decelerated motion. One of the reasons for this is that in the Tamm formula (4.3) corresponding to $\beta n > 1$, the motion interval was taken to be to be equal to z_f which is slightly larger than the distance passed by a charge from the space point where $\beta = \beta_0$ to the space point where $\beta = c/n$. More important is the constancy of a charge velocity implied by the Tamm formula.

In Fig.6, there are shown dependences $dN/d\lambda$ as a function of the initial kinetic energy T for various wavelengths λ. We observe that these dependencies are almost linear. The comparison with the Tamm formula (dotted lines) is presented in Fig. 7. The integral number of photons emitted in the wavelength interval (λ_1, λ_2) as a function of an initial kinetic energy is given by

$$N(T) \equiv N(\lambda_1, \lambda_2, T) = \int_{\lambda_1}^{\lambda_2} \frac{dN}{d\lambda} d\lambda, \tag{4.5}$$

where $dN/d\lambda$ is given by (4.3). In Fig. 8, the solid curve corresponds to $N(T, \lambda_1, \lambda_2)$ with $\lambda_1 = 2.144 \cdot 10^{-5} cm$ and $\lambda_2 = 5.893 \cdot 10^{-5} cm$. It is obtained by the integration over λ curves with fixed λ shown in Fig.6. In the same Fig. 8, there are presented results of calculations of Ref. [19] (dotted curve) and Ref. [20] (dashed curve). We

observe the sharp disagreement with our calculations.
The idea of calculations made in [19, 20] originates from the method suggested by Cherenkov [21] who begins with the Tamm-Frank formula

$$\frac{d\mathcal{E}}{dz} = \int f(\omega)d\omega, \tag{4.6}$$

describing the energy losses per unit length on the surface of a cylinder coaxial with the charge motion axis. Equation (4.5) is related to an infinite charge motion with a constant velocity. $f(\omega)$ entering into (4.6)

$$f(\omega) = \frac{d^2\mathcal{E}}{dzd\omega} = \frac{e^2\omega}{c^2}(1 - \frac{1}{\beta^2 n^2})$$

is the energy loss per unit length per unit frequency.

Similar expression for the number of photons emitted per unit length looks like

$$\frac{dN}{dz} = \int N(\omega, z)d\omega, \tag{4.7}$$

where

$$N(\omega, z) = \frac{d^2N}{dzd\omega} = \frac{\alpha}{c}(1 - \frac{1}{\beta^2 n^2}), \quad \alpha = \frac{e^2}{\hbar c}$$

is the number of photons emitted per unit length unit per unit frequency. The number of photons emitted on the interval z_1, z_2 of the cylinder surface in the frequency interval ω_1, ω_2 is given by

$$N = \int_{z_1}^{z_2}\int_{\omega_1}^{\omega_2} N(\omega, z)d\omega dz. \tag{4.8}$$

Now, Cherenkov assumed that the charge velocity entering into $f(\omega)$ and $N(\omega, z)$ is a function of z. He integrated (4.8) from z_1, for which the charge velocity is equal to the initial velocity to z_2, for which the charge velocity is equal to the threshold velocity $1/n$ (in fact, only for that interval of velocities, Eqs.(4.6) and (4.7) are valid). The identification of the (z_1, z_2) interval with the charge path is not very clear to us, since Eq. (4.6) was obtained under the assumption of unbounded charge motion with a constant velocity. On the other hand, Eqs.(4.3) and (4.5) unambiguously define the number of photons with a given λ and the number of photons in the (λ_1, λ_2) interval, resp., passing through the sphere surrounding the charge path.

4.1 Numerical calculations for the electrons emitted by ^{40}K

So far, we evaluated distributions of the energy and the number of photons radiated by an electron moving in water. But the electrons emitted by real sources have definite energy distributions, As an example, the number of electrons per unit kinetic

energy dN_e/dT (in arbitrary units) arising in the β-decay of ^{40}K have the kinetic energy distribution shown in Fig. 9. The corresponding data were taken from [22] for $0.1MeV < T < 1.1MeV$. We extrapolated them to the $1.1MeV < T < 1.3MeV$ interval. To avoid the use of arbitrary units, we normalize dN_e/dT as follows

$$(\frac{dN_e}{dT})_n = \frac{dN_e}{dT} / \int dT \frac{dN_e}{dT}. \tag{4.9}$$

The integral entering into (4.9) is equal to 897.8. Obviously, $(dN_e/dT)_n$ is normalized to unity:

$$\int dT (\frac{dN_e}{dT})_n = 1.$$

If we multiply $(dN_e/dT)_n$ given by (4.9) by $dN/d\lambda$ defined by (4.3), we obtain the number of photons emitted by the decelerated electron (with the initial kinetic energy T) arising from the β-decay of ^{40}K. Conditionally, we denote it by $d^2N/d\lambda dT$. We apply this procedure to the curves shown in Fig. 6. The results of calculations are shown in Fig. 10. Finally, for the number of photons emitted by the decelerated electron in the wavelength interval (λ_1, λ_2) arising from the β-decay of ^{40}K, one finds

$$\frac{dN(T)}{dT} \equiv N(\lambda_1, \lambda_2, T) = \int_{\lambda_1}^{\lambda_2} d\lambda \frac{d^2N}{d\lambda dT}. \tag{4.10}$$

For $\lambda_1 = 2.144 \cdot 10^{-5} cm$ and $\lambda_2 = 5.893 \cdot 10^{-5} cm$, $dN(T)/dT$ given by (4.10) is shown in Fig. 11. The total number of photons emitted by decelerated electrons arising from the β-decay of ^{40}K is obtained by integration of $N(T)$ given by (4.10) over all kinetic electron energies:

$$N = \int_{T_{min}}^{T_{max}} \frac{dN(T)}{dT} dT, \quad T_{min} = 0.1MeV, \quad T_{max} = 1.3MeV.$$

For the distribution $dN(T)/dT$ presented in Fig. 11, this number is about 25. It corresponds to the energy per one decay averaged over the β-spectrum.

5 Conclusion

We considered the general properties of the Cherenkov radiation in medium arising from instant acceleration of electron followed by its smooth deceleration. The motion begins from the state at rest. Then, an electron exhibits an instantaneous acceleration up to reaching the velocity v and moves with deceleration up to reaching the state at rest. The ranges of electrons were taken from Tables. In fact, this is a typical situation in nuclear water reactors. Physically, this problem can be realized

in the β-decay of an atom imbedded into water with the subsequent deceleration of the emitted electron. This consideration is exact, as far as we do not take into account the multiple electron scattering on the medium inhomogenuities. The analytic expression for the radiation intensity is found when the condition $\lambda z_f^2/R << 1$ (λ, z_f and R are the wavelength, the electron range and the observation distance, resp.) is fulfilled. However, in realistic cases, this condition is strongly violated [12]. Thus, we decided to limit ourselves to pure numerical results.

We briefly summarize the main results obtained:

1. The dependence of the radiation propagation on the electron velocity does not follow the classical law $\cos\theta = 1/\beta n$. The agreement is satisfactory for $\beta \approx 1$ and fails at the Cherenkov threshold $\beta = 1/n$.
2. The dependence of the radiation intensity on the electron velocity has no sharp threshold at $\beta = 1/n$. The change of intensity near the threshold is more smooth than that described by the Tamm formula.
3. The absolute value of the emitted photon number is much smaller than that given by the Tamm formula. A possible reason is that the Tamm problem contains two instantaneous jumps of the charge velocity (at the beginning and termination of motion), while there is only one instantaneous jump of the charge velocity (at the beginning of motion) for the treated deceleration motion. It is known that an interference of bremsstrahlungs arising from two instantaneous jumps of velocities in Tamm's problem leads to the increasing of the total radiation intensity by 4 times [8]. Other possible reasons for this are that a rather simplified law (2.5) for the velocity losses was used and that it was not taken into account the multiple scattering.

The results of this investigation show that charge acceleration and deceleration play an important role in the consideration of the Vavilov-Cherenkov effect, in accordance with Vavilov predictions [7] made in 1934.

Table 1: Initial electron kinetic energies T, velocities β and corresponding to them electron ranges Z_f in water taken from Tables [16]

T,MeV	β	Z_f,cm
0.1	0.5482	$1.400 \cdot 10^{-2}$
0.2	0.6953	$4.400 \cdot 10^{-2}$
0.3	0.7765	$8.263 \cdot 10^{-2}$
0.5	0.8629	$1.735 \cdot 10^{-1}$
1.3	0.9594	$5.890 \cdot 10^{-1}$
2.0	0.9791	$9.613 \cdot 10^{-1}$
5.0	0.9957	2.499
10.0	0.9988	4.880

Table 2: Wavelengths λ, corresponding to them refractive indices n and threshold Cherenkov velocities β_c for water at 20°C

λ, 10^{-5}cm	$n(\lambda)$	$\beta_c = 1/n(\lambda)$
2.144	1.4032	0.7127
3.034	1.3581	0.7363
4.047	1.3428	0.7447
5.893	1.3330	0.7502
6.780	1.3308	0.7514

Table 3: Positions of angular distributions maxima θ_m for the treated deceleration motion and the Cherenkov angles $\theta_{Ch} = \arccos(1/\beta n)$

T,MeV	$\lambda, 10^{-5}$cm	θ_m,deg	θ_{Ch},deg
1.3	2.144	41.8	42.0
1.3	5.893	38.1	38.6
1.3	6.708	38.0	38.4
0.3	2.144	22.3	23.4
0.3	5.893	12.0	15.0
0.3	6.708	11.4	14.6

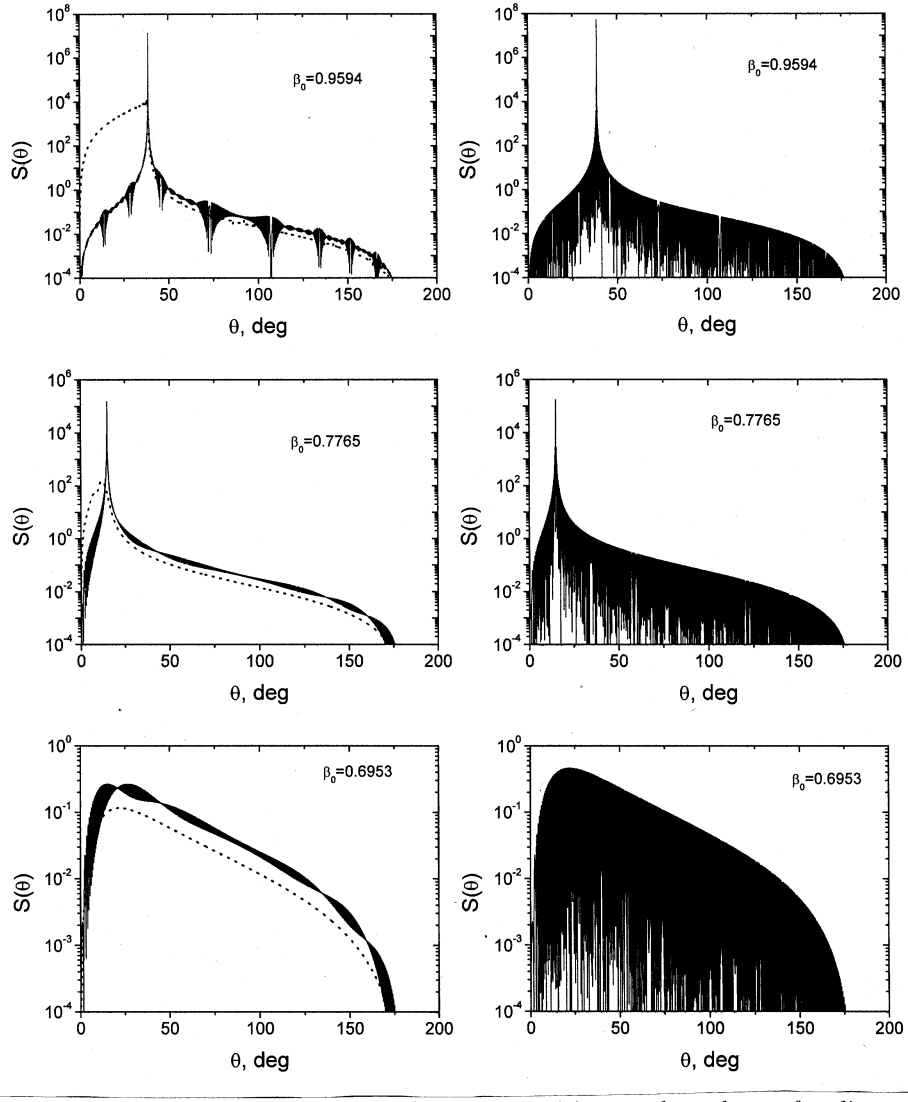

Fig. 1. Left column: The angular radiation intensities on the sphere of radius $r = 100cm$ corresponding to the decelerated charge motion (dotted lines). Tamm intensities shown by solid lines were obtained by averaging over 5 neighboring points (to make possible comparison with decelerated motion intensities). Right column: Non-averaged Tamm's intensities.
The wavelength, refractive index and Cherenkov threshold are $\lambda = 5.893 \cdot 10^{-5}cm$, $n = 1.333$ and $\beta_c = 1/n = 0.7502$, resp. The electron ranges are: $z_f = 0.589cm$ for $\beta_0 = 0.9594$, $z_f = 8.263 \cdot 10^{-2}cm$ for $\beta_0 = 0.7765$ and $z_f = 4.4 \cdot 10^{-2}cm$ for $\beta_0 = 0.6953$.

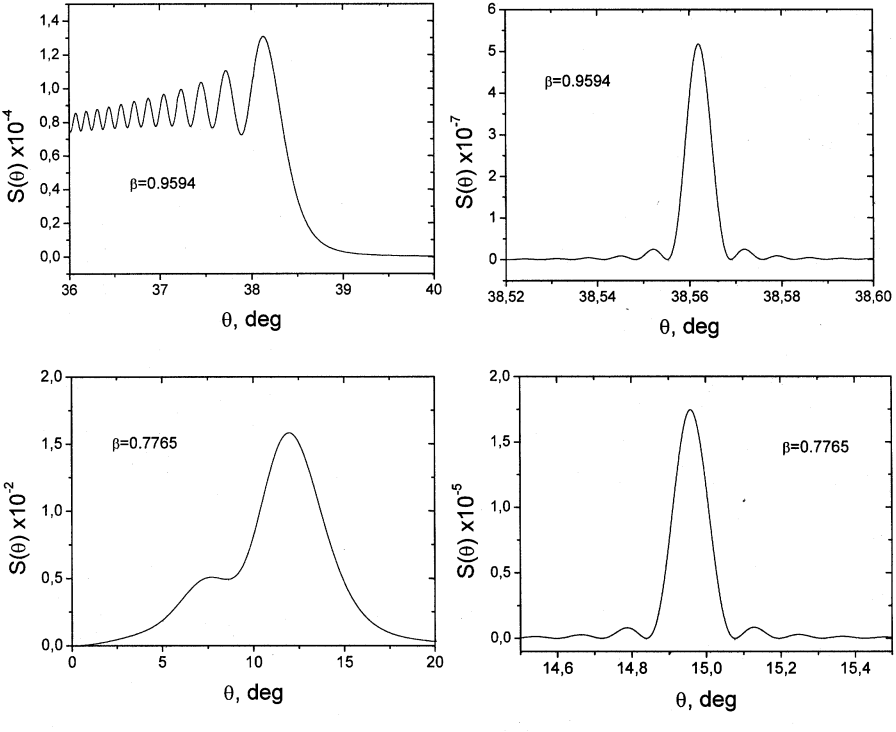

Fig.2: The same as in Fig.1, but for a smaller θ interval. Left column: angular intensities for the treated decelerated charge motion. Right column: Tamm angular intensities.
The main maxima of the radiation intensity for decelerated motion are at $\theta_m = 38.1^0$ for $\beta_0 = 0.9594$ and at $\theta_m = 12^0$ for $\beta_0 = 0.7765$. The corresponding maxima for the Tamm intensity are at $\theta_c = 38.6^0$ and $\theta_c = 15.5^0$, resp. Other parameters are the same as in Fig.1.

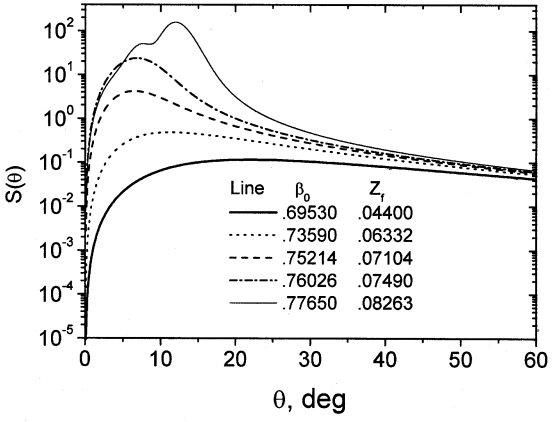

Fig.3: Angular radiation intensities corresponding to decelerated motion for various initial velocities β_0 in the neighborhood of the Cherenkov threshold $\beta_c = 0.7502$. The wavelength $\lambda = 5.893 \cdot 10^{-5} cm$. It is seen that intensities change rather slowly near the Cherenkov threshold. Other parameters are the same as in Fig.1.

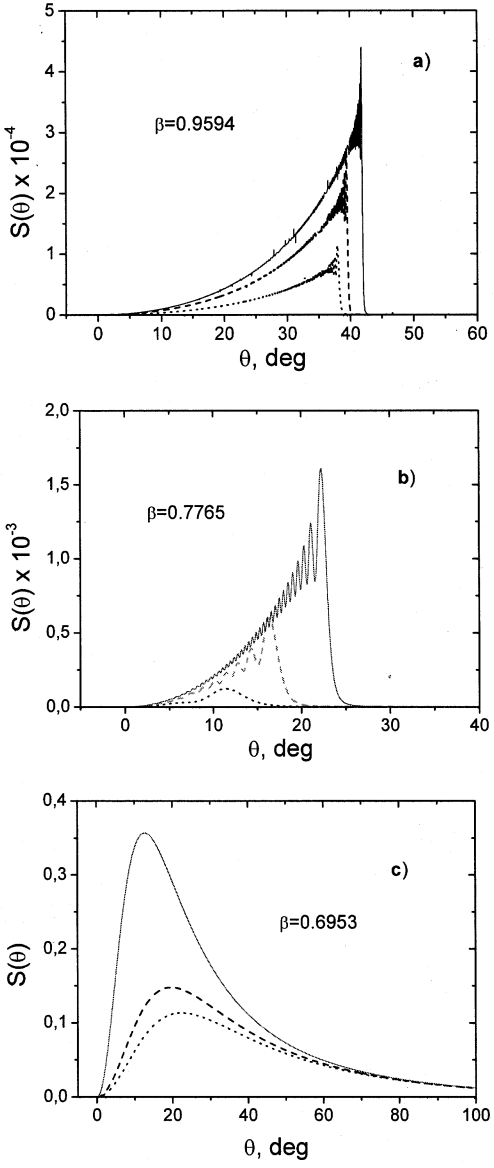

Fig.4: Angular radiation intensities corresponding to decelerated motion for different wavelengths and initial velocities: $\beta_0 = 0.9594$ (a), $\beta_0 = 0.7765$ (b) and $\beta_0 = 0.6953$ (c). Solid, broken, and dotted lines correspond to $\lambda = 2.144 \cdot 10^{-5} cm, n = 1.4032$, $\lambda = 3.034 \cdot 10^{-5} cm, n = 1.3551$ and $\lambda = 6.780 \cdot 10^{-5} cm, n = 1.3308$, resp. Other parameters are the same as in Fig.1.

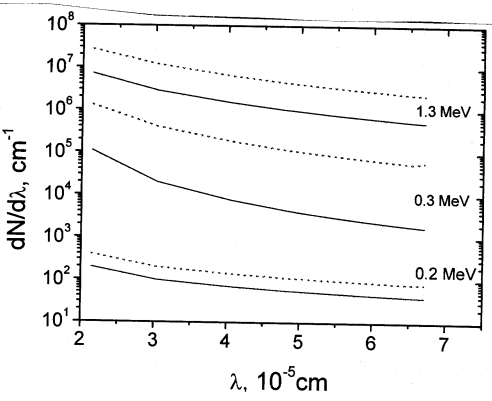

Fig. 5: The number of photons per unit wavelength as a function of the observed wavelength for a fixed initial velocity. Solid and dotted lines correspond to the decelerated motion and the Tamm formula (4.4).

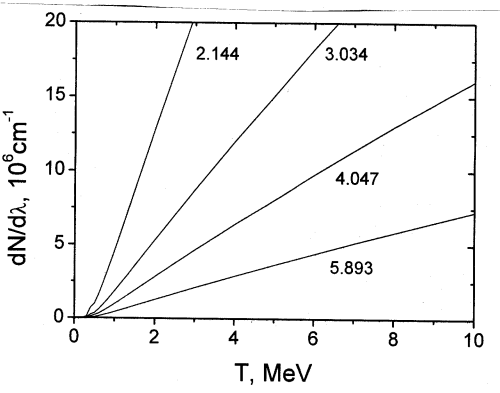

Fig.6: The number of photons per unit wavelength as a function of the initial kinetic energy for the fixed wavelengths $\lambda = 2.144 \cdot 10^{-5} cm, n = 1.4032$ (curve 1), $\lambda = 3.034 \cdot 10^{-5} cm, n = 1.3557$ (curve 2), $\lambda = 4.047 \cdot 10^{-5} cm, n = 1.3428$ (curve 3) and $\lambda = 5.893 \cdot 10^{-5} cm, n = 1.333$ (curve 4) for the treated deceleration motion (solid curve). We observe that the dependence on the initial kinetic energy is almost linear.

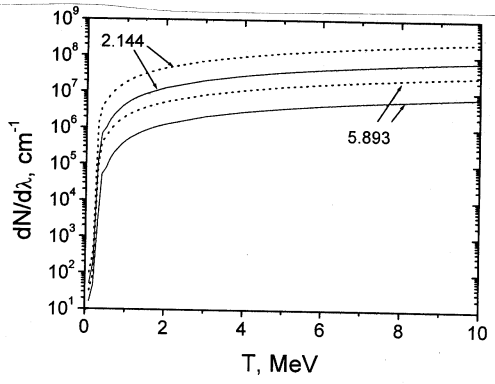

Fig.7: Comparison $dN/d\lambda$ for the treated decelerated motion (solid lines) with that given by the Tamm formula (4.4) (dotted lines) for $\lambda = 2.144 \cdot 10^{-5} cm, n = 1.4032$ and $\lambda = 5.893 \cdot 10^{-5} cm, n = 1.333$.

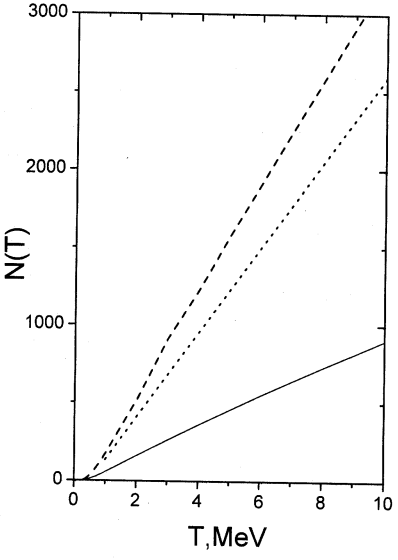

Fig. 8: The integral number of photons emitted in the region of visible light ($2.144 \cdot 10^{-5} cm \leq \lambda \leq 5.893 \cdot 10^{-5} cm$). Solid curve corresponding to the treated decelerated motion was obtained by integrating over λ curves presented in Fig. 6. Dotted and broken lines correspond to the data taken from Refs. [19] and [20], resp.

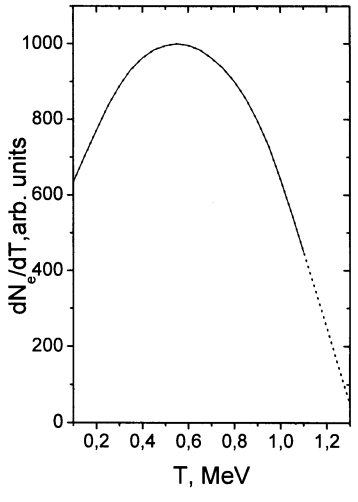

Fig. 9: The β spectrum of ^{40}K. Solid and broken parts of the curve correspond to experimental data taken from [22] and to their extrapolation, resp.

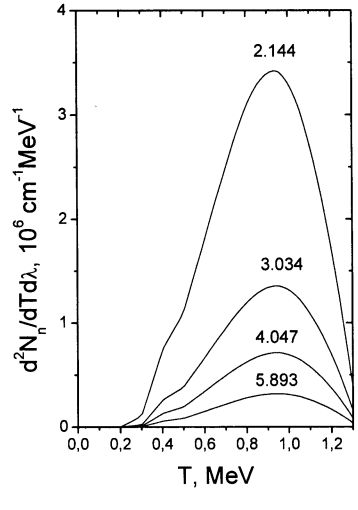

Fig. 10: Distributions of the photon number with a fixed wavelength emitted by decelerating electrons originating from β-decay of ^{40}K in water as a function of kinetic energy. These distributions were obtained by folding the curves shown in Fig. 6 with the β-decay spectrum of ^{40}K presented in Fig. 9.

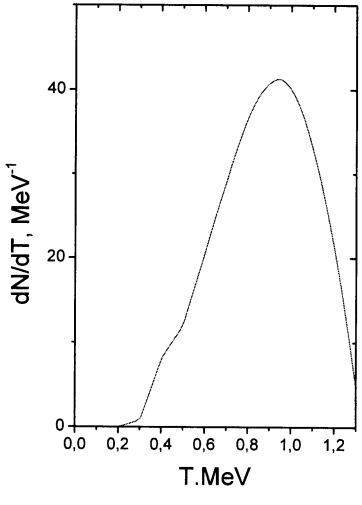

Fig. 11: The integral number of photons emitted in the region of visible light ($2.144 \cdot 10^{-5} cm \leq \lambda \leq 5.893 \cdot 10^{-5} cm$) as a function of kinetic energy. This curve is obtained by integrating curves shown in Fig. 10 over λ. The total number of photons emitted by decelerated electrons emitted by ^{40}K decaying in water is obtained by integrating the curve shown in this figure over T. It equals 25.

References

[1] Frank I.M., 1988, Vavilov-Cherenkov Radiation (Moscow, Nauka), In Russian.

[2] Tamm I.E., 1939, J.Phys. USSR, 1, 439.

[3] Aitken D.K. et al., 1963, Proc. Phys. Soc.. 82, 710.

[4] Kobzev A.P., Frank I.M., 1981, Yad. Fiz., 34, 125.

[5] V.P. Zrelov et al., 1983, NIM, 215, 146,

[6] Ruzicka J. and Zrelov V.P., 1993, Chech. J. Phys., 43, 551

[7] Vavilov S.I., 1934, Dokl. Akad, Nauk, 2, 8, 457.

[8] Zrelov V.P., Ruzicka J., 1989, Chech.J.Phys. B, 39, 368.

[9] Zrelov V.P., Ruzicka J., 1992, Chech.J.Phys., 42, 45.

[10] Afanasiev G.N., Beshtoev Kh. and Stepanovsky Yu.P., 1996, Helv. Phys. Acta, 69, 111-129; Afanasiev G.N., Kartavenko V.G. and Stepanovsky Yu.P., 1999, J.Phys. D, 32, 2029.

[11] Kuzmin E.S. and Tarasov A.V., 1993, JINR Rapid Communications, 4[61]-93, 64 (Dubna, 1993);

[12] Afanasiev V.M., Shilov V.M., 2000, J. Phys.D, 33, 2931.

[13] Krupa L., Ruzicka J. and Zrelov V.P., 1995, JINR Preprint P2-95-281.

[14] Afanasiev V.M., Shilov V.M., 2000, Physica Scripta, 63, 326;

[15] Berger M.J. and Seltzer S.M., 1964, Tables of energy losses and ranges of electrons and positrons, In Studies in penetration of charged particles in matter, Publ. No 1133, p.249 (Natl. Acad. Sci.and Natl. Research Council, Washington).

[16] Landau L.D. and Lifshitz E.D., 1992, Electrodynamics of Continuous Media (Oxford, Pergamon).

[17] Tables of physical quantities (Ed. I.K. Kikoin), 1976 (Atomizdat, Moscow), in Russian.

[18] Breton D., 1955, Report C.E.A. No 1198, Saclay.

[19] Myasnik M.N., Skvortzov V.G., Sokolov V.A., 1985, Photobiological Aspects of the Radiation Damage of Cells, p.139, (Moscow, Energoatomizdat), In Russian.

[20] Cherenkov P.A., 1944, Trudy FIAN, vol.2, No 4, pp. 3-62, In Russian.

[21] Leutz H., Schultz G., Wenniger H., 1965, Z.f. Physik, 187, 151.

Received by Publishing Department
on October 3, 2001.

Афанасьев Г.Н., Картавенко В.Г., Зрелов В.П. Е2-2001-207

Особенности излучения типа черенковского от замедляемого электрона, возникающего при β-распаде в воде

Рассмотрены свойства излучения, возникающего при мгновенном ускорении заряда вплоть до достижения им скорости, большей скорости света в веществе, и последующем его замедлении вплоть до полной остановки. Получена общая формула, описывающая это излучение. Используя ее, мы вычислили угловые и спектральные распределения, а также число испущенных фотонов в зависимости от начальной энергии электрона (максимальная энергия 10 МэВ). Эти распределения могут быть использованы для оценки черенковского излучения в ядерных реакторах с тяжелой водой. Вычислен спектр черенковского излучения, возникающего при β-распаде ^{40}K ($E_{\max} = 1{,}3$ МэВ). В общем случае угловые распределения не имеют максимума при $\cos\theta = 1/\beta_n$. Сдвиг максимума более выражен вблизи черенковского порога $\beta_n = 1$. Число испущенных фотонов примерно в 3,5 раза меньше, чем по классической формуле, также учитывающей ускорение. Мы связываем это с наличием двух мгновенных скачков скоростей в исходной задаче Тамма и только одного скачка в данном подходе. Это приводит к отсутствию интерференции между тормозными излучениями, испущенными в начале и в конце движения. Данная работа указывает на необходимость пересмотра основ теории излучения Вавилова–Черенкова.

Работа выполнена в Лаборатории теоретической физики им. Н.Н.Боголюбова ОИЯИ.

Препринт Объединенного института ядерных исследований. Дубна, 2001

Afanasiev G.N., Kartavenko V.G., Zrelov V.P. E2-2001-207

Peculiarities of the Cherenkov-Like Radiation from the Decelerated Electron Arizing from the β-Decay in Water

We considered radiation arising from an instantaneous charge acceleration up to reaching the velocity greater than the light velocity in medium and its smooth deceleration up to its complete stopping. General formula for the radiation arising from such a charge motion is obtained. Using it, we evaluated the angular frequency distributions of the radiation and the number of emitted photons as a function of the initial electron energy (the maximal energy is 10 MeV). They may be used for the evaluation of Cherenkov radiation in nuclear reactors with heavy water. We evaluated the spectra of the Cherenkov radiation for the decelerated electrons arising from the β-decay of ^{40}K ($E_{\max} = 1.3$ MeV) in water. In general, the angular distributions do not have maximum at $\cos\theta = 1/\beta_n$. The shift of maximum is more pronounced near the Cherenkov threshold $\beta_n = 1$. The number of photons is by 3.5 times smaller than the one given by the classical Tamm formula which also takes into account the deceleration of electrons. We associate this disagreement with the fact that there are two jumps of a charge velocity (at the beginning and termination of motion) in the original Tamm problem, while there is only one velocity jump (at the beginning of motion) in the present consideration. Correspondingly, there is no interference of bremsstrahlung waves emitted at the beginning and termination of a charge motion. This contribution points out to the necessity to reconsider the main postulates of the Vavilov–Cherenkov effect.

The investigation has been performed at the Bogoliubov Laboratory of Theoretical Physics, JINR.

Preprint of the Joint Institute for Nuclear Research. Dubna, 2001

Макет Т.Е.Попеко

Подписано в печать 14.11.2001
Формат 60 × 90/16. Офсетная печать. Уч.-изд. л. 2,63
Тираж 425. Заказ 52952. Цена 3 р. 15 к.

Издательский отдел Объединенного института ядерных исследований
Дубна Московской области